RESEARCH ARTICLE OPEN ACCESS

Experimental Investigation of Jet Impingement Cooling On a Ribbed Surface with Holes

Kartik Jujare[1], Shashank Kumat, Akash Thawkar
(Department of Mechanical Engineering, MIT Academy of Engineering Alandi (D), Pune University - 412105)

ABSTRACT
Jet impingement has found applications in many processes where there is a need for higher heat transfer The paper reports the results of experimental investigations of the flow and heat transfer from a triangular ribbed heated plate with holes, impinged by a round jet in a confined case built around the plate. The parameters varied are heat flux, ratio of the distance of the nozzle from the plate to the diameter of the nozzle and flow rate of air. These values are further processed to calculate the Reynolds number, heat transfer coefficients and consequently the Nusselt numbers for each combination.

Keywords **–** Jet impingement, Reynolds number, Triangular Ribbed surface.

I. Introduction

The jet impingement configuration is applied to many processes, especially where there is a need for high transfer of the heat generated such as in applications concerning electronic cooling. Prior studies have focused their attention on a variety of parameters *i.e.* variation in the nozzle geometry, Reynolds number, angle of incidence and the geometry configuration. Narayanan *et. al.* [1] studied the mechanics of an impinging slot jet flow concluding that the mean and RMS – averaged fluctuating surface pressure, and local heat transfer coefficient peaked at the impinging region and decreased monotonically in the wall bounded flow past impingement . The study also tabulates prior important studies and their variation parameters.

Shyy woei *et.al* [2] studied the heat transfer characteristics of impinging a jet onto concave and convex dimpled surfaces with effusion. Among other geometries studied, Yan and Mei [3] examined the angled rib effects by considering both continuous and broken V-shaped configurations with different exit flow orientations.

Katti and Prabhu [4] in their pursuit to understand and enhance the heat transfer in the detached rib configuration found, contrary to results of the smooth surface, that there is a continuous increase in the heat transfer coefficient from the stagnation point in the stagnation region.

Rallabandi et. al. [5] studied the heat transfer characteristics of both jet impingement and channel flow conditions. The range of the Reynolds number for the flow was 5000 to 40000. The study was also made on the heat transfer characteristics of inline and staggered ribs.

In yet another study, Duda et al. [6] concluded that when a cylindrical pedestal is placed the flow quickly separates over the pedestal edge leading to three distinct regions of the wall jet. There is a recirculation region at the base of the pedestal, a separation zone where flow detaches from the pedestal surface and does not reattach downstream (for low H/d spacing), and a region of separated flow which reattaches after the pedestal boundary and forms the wall jet.

Donovana and Murray [7] in their work studied the effects of rotational motion provided to the Al-foam which was being studied for heat transfer.

In view of these studies, geometry with triangular ribs in parallel orientation was manufactured, with holes drilled between the ribs. The aim was to understand the effect of holes on the air flow patterns and heat transfer characteristics in the enclosure.

II. Experimental setup

The impinging air jet is issued from a blower system which can deliver a maximum air flow of 50 cfm. The nozzle is constructed from a solid nylon pipe. It is made convergent and curved smoothly which allows rapid acceleration of fluid without the occurrence of flow separation. Therefore, uniform velocity profile associated with relatively low turbulence intensity across the nozzle width at the exit is obtained. The jet velocity is measured with a calibrated Orifice meter. The flow can be regulated by a flow regulator on the blower or a dimmerstat. The manual regulator is kept fully open throughout the experiment. The measurement of the velocity is in congruence with the method followed generally.

$$V_{orifice} = C_v \cdot \sqrt{2gh_{mano}} \quad (1)$$

$A_{orifice} \times V_{orifice} = A_{nozzle} \times V_{nozzle}$ (2)

Diameter of nozzle exit is 26.7 mm and length being 80 mm.

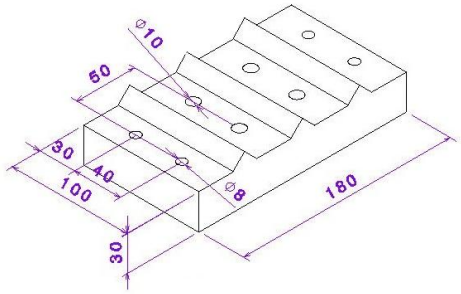

Figure 1 Schematic of Target plate

The schematic of the target plate is shown in Fig. 1. It is 10 cm wide and 18 cm long. There are three 10mm high and a base of 20 mm triangular rib elements. The target plate consists of 8 holes which act as the sole exit route for the spent air. It houses a 3 mm thin heater pad, a 5 mm thin Asbestos sheet and another 5 mm steel plate is fastened to the target plate with the help of bolts to minimize the heat loss. The eight holes extend through the heater, asbestos sheet and the MS plate. The heater wires (nichrome) are placed carefully so as to avoid being exposed directly to air. The target plate can be heated by passing electric current through the wires cased in a pad. All the ribs are equally spaced. To account for the additional radiation heat loss directly from the asbestos sheet, the total heat loss to the surroundings is estimated by assuming the heat transfer co-efficient as 10.

$Q_{generated} = V.I$ (3)

$Q_{loss} = h_{bottom} \times A_{bottom} \times (T_{bottom} - T_{ambient})$ (4)

To ensure that the heater pad is heated uniformly, the entire heater wires inside the heater is arranged in circular fashion. With the desired voltage V and current I passing through the thin heater pad, the heat flux along the surface can be calculated and is equal to VI/A, where A is the area of the top surface of the target plate excluding the holes. The local heat Transfer coefficients were determined with the following equations:

$Q_{actual} = Q_{total} - Q_{loss}$ (5)

$q_{actual} = Q_{actual} / A_{top}$ (6)

$$h_{actual} = \frac{qactual}{Tsurface - Tinlet} \quad (7)$$

The enclosure of the setup, which houses the target plate and the collapsible roof, is made up of two materials. Polycarbonate sheet (k = 0.19 W/mK) has been used on two sides to provide visibility inside the enclosure and plywood (k = 0.13 W/mK) on the other two sides. The enclosure is insulated at the bottom of the vertical walls with neoprene rubber sheets (k = 0.19 W/mK) which is glued so that the heat loss from the vertical walls of the target plate is reduced. The enclosure dimension is made slightly larger than the target plate. The enclosure supports a collapsible roof which has the nozzle fixed to it. The space between the enclosure and the internally sliding roof is made air tight with the help of rubber sheets.

Figure 2 Enclosure assembly

The target plate is mounted on an MS plate which has its central portion cut in a rectangular fashion just enough to support the target plate as well as to allow for the spent air to pass out to the atmosphere (different from the one used to bolt the heater assembly). It is 5 mm thick and saves the user from having to handle the hot target plate. This also serves the purpose of varying the height by moving it along 4 rods which are bolted to the stand.

The plastic pipe which delivers the air is not glued to the L-joint as seen in Fig 2 to allow for flexibility while changing the height of the enclosure.

Power is supplied from a regulated AC power supply. The voltage and current across the heater is measured by a digital voltmeter ammeter. All the temperature signals are acquired with a help of a temperature detector. The temperature is measured using Fe-K thermocouples positioned at five locations- (I) to measure the inlet air temperature (II) placed directly below the exit hole. (III) To measure surface temp the first rib of the plate. (IV) Placed below the heater assembly to calculate the heat loss (V) to measure the atmospheric temperature. The thermocouple wires are extricated carefully from slots made into the rubber sheets.

The Nusselt number for the heat transfer was calculated by

$$Nu = \frac{hd}{k} \quad (6)$$

III. Observations

The observations were made by varying three parameters, namely, Heat flux, H/d ratio, Reynolds's number. Table 1 shows the values for varying H/d ratio and flux for constant Reynolds number of 18300.

Table 1 The range of values of parameters

Sl. no.	Parameters	Range of values studied
1.	Reynolds number	13700, 15900, 18300
2.	H/d ratio	4.02, 8.02, 11.02
3.	Flux (W/m^2)	2812.25,3696.88,4802.119, 5956.68, 7286.54

Various non-dimensional and dimensional parameters were calculated, including heat transfer coefficient and Nusselt number.

Table 2
Results obtained for Reynolds number of 18300

Sl. no.	H/d ratio	V(volts)	I(amp)	Flux(W/m^2)	T_{atmo}	T_{inlet}	T_{exit}	T_{bottom}	$T_{surface}$
1.	4.02	130.99	0.7467	2812.25	28	34	40	56	45
2.		150.12	0.8565	3696.88	28	36	40	59	47
3.		170.725	0.9783	4802.19	28	36	41	62	50
4.		190.75	1.0861	5956.68	28	36	43	67	53
5.		211.7	1.1971	7286.54	28	37	45	73	56
6	8.02	130.99	0.7467	2812.25	28	36	41	55	47
7.		150.12	0.8565	3696.88	28	35	44	63	50
8.		170.725	0.9783	4802.19	28	35	47	70	54
9.		190.75	1.0861	5956.68	28	34	46	80	56
10.		211.7	1.1971	7286.54	28	34	48	90	62
11.	11.02	130.99	0.7467	2812.25	28	36	41	54	46
12.		150.12	0.8565	3696.88	28	36	41	59	49
13.		170.725	0.9783	4802.19	28	37	43	67	53
14.		190.75	1.0861	5956.68	28	37	45	73	57
15.		211.7	1.1971	7286.54	28	37	46	91	65

The procedure to note down readings was as follows: The heater and the blower were switched on at the right voltage and was allowed to run till steady state is reached. The readings of the temperature indicator were noted once it reached the steady state position. While evaluating the observations following data were considered,

Table 3
Values of parameters considered for calculation

Sl. no.	Parameter	Value
1.	Density of air	1.225 kg/m^3
2.	Dynamic viscosity of air	17.89 x 10^{-6} kg/ms
3.	Thermal conductivity of air	0.0242 W/mk
4.	Coefficient of velocity	0.92
5.	A_{top} for q_{actual}	0.02 m^2
6.	A_{bottom} for q_{loss}	0.01478 m^2

IV. Calculations

The methodology to calculate the heat transfer coefficient and Nusselt number is shown in Appendix-I. Table 4 shows the values of HTC and Nusselt number against the flux and H/d ratio provided. The heat transfer coefficient for the loss was assumed to be 10 W/m^2K.

V. Analysis

In the present study, the parametric variation of the heat transfer coefficient shows an increasing trend with the increase in the Reynolds number. Similarly the Nusselt number can generally be seen to be increasing with the corresponding increase in the Reynolds number and the heat flux evident from Fig 3, 4 and 5.

The effect of the variation of the H/d is as follows.

The higher H/d ratio causes high entrailment compared to lower H/d ratios.

Table 4
Nusselt number for Reynolds number of 18300.

Sl. no.	H/d ratio	Flux (W/m^2)	Heat transfer coefficient (W/m^2K)	Nusselt number
1.	4.02	2812.25	425.7811	469.76671
2.		3696.88	563.6181	621.8431
3.		4802.19	578.5538	638.32177
4.		5956.68	592.3805	653.57685
5.		7286.54	649.4081	716.49569
6.	8.02	2812.25	426.4529	470.50793
7.		3696.88	411.3493	453.84403
8.		4802.19	423.1912	466.90933
9.		5956.68	453.3818	500.21872
10.		7286.54	436.183	481.24321
11.	11.02	2812.25	469.8372	518.37406
12.		3696.88	476.9076	526.17493
13.		4802.19	503.9252	555.9836
14.		5956.68	501.3064	553.09429
15.		7286.54	435.9191	480.95201

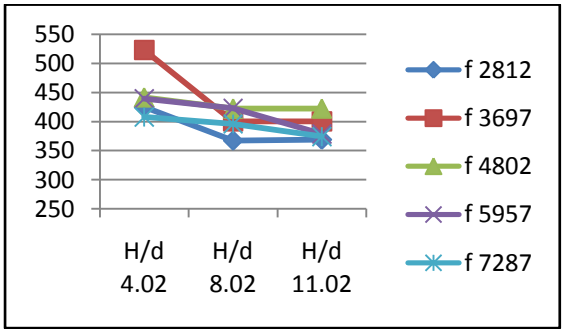

Figure 3 Values of Nusselt number for Reynolds number 13700

For higher H/d ratios the momentum exchange observed between impinging and quiescent fluid implies that the impinging jet becomes broader and spreads over more surface area which also causes possible vortex formation. However in case of less H/d ratio same amount of fluid spreads over less surface area thus causing higher heat transfer rate.

The oddity to understand would be the increase in the inlet temperature of air. This increase could be attributed in a small way to the heat gain from the blower but majorly because of the rise of hot air from the enclosure towards the inlet thermocouple.

Secondly, we observe that the heat transfer coefficients remain more or less the same because of the simple reason that the assembly is housed inside an enclosure which allows the air to exit in only one way that is through the holes in the target plate.

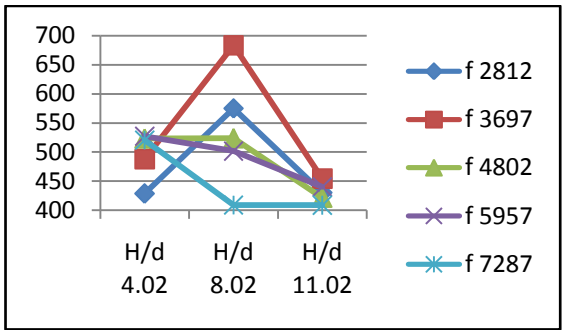

Figure 4 Values of Nusselt number for Reynolds number 15900

The incoherence in the readings can be attributed to the instabilities arising because of the interaction between natural and forced convection.

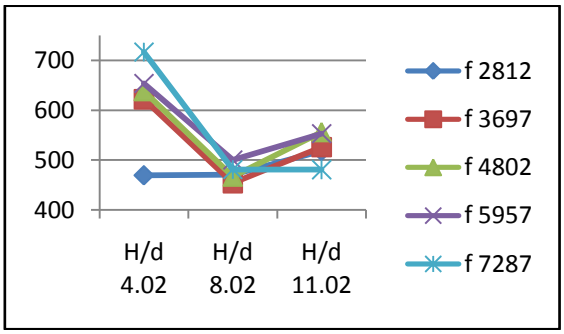

Figure 5 Values of Nusselt number for Reynolds number 18300

VI. Conclusion

In this work effect of Reynolds number, heat flux, and H/d ratio on the local Nusselt number is investigated. It was carried out on a triangularly ribbed target plate with holes. As the bottom grill is the only exit, there is an increase in the heat transfer coefficient.

The following can be concluded from the study

- That there is an increase in the heat transfer as the H/d ratio decreases.
- With a general increase in the heat flux there is a general rise in the heat transfer rate.
- An increase in the Reynolds number also increases the heat transfer rate for constant heat flux and H/d ratio

VII. Acknowledgement

The authors would like to thank Dr. Mayur Bhoite for his support and MIT Academy of Engineering, Alandi for providing us with the opportunity and space to conduct the study. We also thank Ms. Sayali Wable for her help in putting together the Experimental setup.

References

[1] V. Narayanan, J. Seyed-Yagoobi, R.H. Page, An experimental study of fluid mechanics and heat transfer in an impinging slot jet flow, *International Journal of Heat and Mass Transfer 47 (2004) 1827–1845*.

[2] Shyy Woei Changa, Hsin-Feng Liou ,Heat transfer of impinging jet-array onto concave- and convex-dimpled surfaces with effusion, *International Journal of Heat and Mass Transfer 52 (2009) 4484–4499*.

[3] W.M. Yan, S.C. Mei, Measurement of detailed heat transfer along rib-roughened surface under arrays of impinging elliptic jets, *International Journal of Heat and Mass Transfer 47 (2004) 5235–5245.*

[4] Vadiraj Katti, S.V. Prabhu, Heat transfer enhancement on a flat surface with axisymmetric detached ribs by normal impingement of circular air jet, *International Journal of Heat and Fluid Flow 29 (2008) 1279–1294*

[5] Akhilesh P. Rallabandi, Dong-Ho Rhee, Zhihong Gao, Je-Chin Han, Heat transfer enhancement in rectangular channels with axial ribs or porous foam under through flow and impinging jet conditions, *International Journal of Heat and Mass Transfer 53 (2010) 4663–4671*

[6] John C. Duda, Francis D. Lagor, Amy S. Fleischer, A flow visualization study of the development of vortex structures in a round jet impinging on a flat plate and a cylindrical pedestal, *Experimental Thermal and Fluid Science 32 (2008) 1754–1758*

[7] Tadhg S. O'Donovana, Darina B. Murray, Fluctuating fluid flow and heat transfer of an obliquely impinging air jet, *International Journal of Heat and Mass Transfer 51 (2008) 6169–6179*

Nomenclature	
$V_{orifice}$	Velocity at orifice
C_v	Coefficient of velocity
H/d ratio	The ratio of the height between nozzle and plate to the diameter of nozzle.
g	Gravitational constant
H_{mano}	Height observed in manometer
A_{bottom}	Area of heater assembly exposed to air for q_{actual}
$A_{orifice}$	Area of orifice opening
A_{nozzle}	Area of nozzle opening
V_{nozzle}	Velocity at nozzle opening
$Q_{generated}$	Total heat generated from the heater
Q_{loss}	Total heat lost from the bottom exposure to air
q_{actual}	Heat actually carried away by jet impingement per unit area
h_{bottom}	Heat transfer coefficient for bottom surface
h_{actual}	Actual heat transfer coefficient
T_{bottom}	Temperature obtained on the bottom surface of target plate
T_{atmo}	Atmospheric temperature

Appendix I

Sample calculation:

$A_{top} = 0.02\ m^2$

$A_{bottom} = 0.01478\ m^2$

$Q_{total} = (V \times I) = 97.81W$

$Flux = \frac{Qtotal}{(Abottom + Atop)} = 2812.25\ W/m^2$

$Q_{loss} = h_{bottom} \times A_{bottom} (T_{bottom} - T_{atmo})$

$= 10 * 0.01478 *(40-28)$

$= 4.1384\ W$

$h_{bottom} = 10\ W/m^2K$ (assumed)

$Q_{actual} = Q_{total} - Q_{loss} = (97.81-4.1384)$

$= 93.6716\ W$

$q_{actual} = Q_{actual}/ A_{top} = 93.6716 /0.02$

$= 4683.5917\ W/m^2$

$q_{actual} = h_{actual}*(T_{surface} - T_{inlet})$

$h_{actual} = q_{actual}/(T_4 - T_1)$

$=4683.5917 /(45-34)$

$= 425.78\ W/m^2 k$

Reynold's number calculation

$V_1 = C_v \sqrt{(2gh_{mano})} = 1.1085$ m/s

$C_v = 0.92$

From Continuity equation: $A_1V_1 = A_2V_2$

$V_2 = 10$ m/s

$Re = (\rho_{air} V_2 D)/\square$

$= (1.225*7.5*0.0267)/(1.79E-05)$

$= 18272$

Nusselt Number calculation

$Nu = (h \times L) / K$

$= (425.78 *0.0267)/(0.0242)$

$= 469.76$